ELSEVIER

Journal of Nuclear Materials 305 (2002) 202–208

journal of nuclear materials

www.elsevier.com/locate/jnucmat

Microstructure and leach rates of apatite glass-ceramics as a host for Sr high-level liquid waste

Yong He [a,*], Weimin Bao [b], Chongli Song [b]

[a] *Materials Science and Chemical Engineering College, China University of Geosciences, 430074 Wuhan, People's Republic of China*
[b] *Nuclear Energy Technology Institute, Tsinghua University, 100083 Beijing, People's Republic of China*

Received 5 November 2001; accepted 10 June 2002

Abstract

An apatite glass-ceramic wasteform with 21 wt% SrO loading was fabricated for immobilizing Sr high-level liquid waste. The normalized leach rates of Sr, K, Mo, Al, P, Si are 6.9×10^{-4}, 1.09×10^{-1}, 2.7×10^{-3}, 3.22×10^{-2}, 2.84×10^{-2}, 3.26×10^{-2} g/m^2 day, respectively. Component Fe in all leachates is not detectable in the 28-day static leaching test procedure in MCC-1. Instead of leaching, component Ca is adsorbed by testing samples. All the component Mo concentrates in the glass matrix of the well crystallized apatite glass-ceramics. For an apatite glass-ceramic wasteform, the optimum microstructure should be one in which poorly crystallized apatite crystallites distribute evenly in the glass phase. Perfect crystallization makes the crystal phase more stoichiometric and significantly changes the composition of the coexisting glass phase in the system, which, in our case, decreases the chemical stability of the apatite glass-ceramics.

PACS: 28.41.Kw

1. Introduction

Glass-ceramics is the third high-level liquid waste (HLLW) wasteform joining the other two, glasses and ceramics. Phosphate glass-ceramics as hosts for HLLW have been paid much less attention compared to silicate and oxide glass-ceramics [1]. The main reason hampering the development of phosphate glass-ceramic wasteforms might be that some metaphosphate glass could usually be found in the glass-ceramics; it is well known that metaphosphate glasse is unstable in water or under damp circumstances. However, two important factors must be considered when fabricating a phosphate glass-ceramic host for HLLWs: one is choosing suitable crystalline phase(s) and the other is designing a glass matrix with high chemical durability. Some phosphate minerals naturally containing radioactive elements have existed in different geological bodies for millions, or even billions of years. Monazite, whose analogue has been employed as a host for HLLWs [1,2], is the best example. Apatite also is a phosphate mineral naturally containing elements in HLLWs [3–5], such as U, Th, Ce, La, Sr, Fe, K, Na, and the like (in solid solution). In order to immobilize ^{90}Sr HLLW partitioned from the kind of HLLW stored in China, a phosphate glass-ceramic wasteform was fabricated, in which apatite was chosen as the main crystalline phase.

2. Experimental procedures

2.1. Formulation of glass-ceramics

^{90}Sr HLLW, one of three HLLW streams produced in the partitioning process [6] established by Nuclear Energy Technology Institute, Tsinghua University, was

* Corresponding author.
E-mail address: heyongyu@263.net (Y. He).

0022-3115/02/$ - see front matter
PII: S0022-3115(02)00920-0

Table 1
Composition of a ^{90}Sr waste stream (g/l)

Atom	g/l
Sr	0.5
Na	0.07
K	0.162
Fe	0.008
Mo	0.007
Cs	0.004
Al	0.008

in a state of nitrate solution. The composition of the waste stream is listed in Table 1. Instead of a real waste stream, we worked on a simulated one in which ^{90}Sr was replaced by its stable isotope and Cs was removed because of its low concentration and similar chemical nature with Na and K.

The composition of the glass precursor and reagents used in the experiments are listed in Table 2. In our experiments, simulated waste components Sr, K, Na, Al, Fe were introduced in their nitrate forms, Mo in ammonium molybdate and P_2O_5, SiO_2 and CaF_2, glass formers and additives, in ammonium dihydrogen phosphate, SiO_2 powder and CaF_2 powder, respectively. Excess Al_2O_3 was added to retard corrosion to Al_2O_3 crucibles. Urea with the same weight as the total reagents was used to destroy those nitrates. All chemicals used were reagent-grade.

A mixture of the ingredients in Table 2 (except CaF_2) was evenly mixed and heated at 550 °C for 30 min to form an oxide powder. Then, the powder and the weighed CaF_2 were mixed together to form one batch of glass precursor in a weight of about 18 g. The batch was melted in an alumina crucible at 1400 °C for about 1 h. After being stirred and refined, the melt was quenched by being poured on a stainless steel plate without annealing. The glass blocks were milk white. Glass-ceramics GC_{825} and GC_{875} were prepared by two stages:

Table 2
Composition of glass precursor and quantities of reagents introduced

Oxide	wt%	Reagent	g
SrO	21.71	$Sr(NO_3)$	8.043
Na_2O	3.46	$NaNO_3$	1.720
K_2O	7.17	KNO_3	2.794
Fe_2O_3	0.37	$Fe(NO_3) \cdot 9H_2O$	0.338
MoO_3	0.55	$(NH_4)_6Mo_7O_{24} \cdot 4H_2O$	0.123
Al_2O_3	12.34	$Al(NO_3)_3 \cdot 9H_2O$	16.486
SiO_2	7.72	SiO_2 powder	1.402
P_2O_5	35.22	NH_4 H_2PO_4	10.352
CaF_2	11.46	CaF_2 powder	2.080
Total	100.00	Total	43.337
		Urea	43.000

first, the glass blocks were heated at 5 °C/min to 650 °C and kept at this temperature for 1 h for nucleation; then, one part of blocks was heated at 2 °C/min to 825 °C and the other to 875 °C and kept at the temperatures for 2 h for crystallization, respectively.

For comparison, the parent glass was chosen for leach tests. In order to obtain glass samples without any cracks during fabrication, the parent glass was annealed at 500 °C for 1 h. However, the XRD pattern for the annealed glass shows that apatite crystallized out of the glass, i.e. an apatite glass-ceramic has formed which we named GC_{500}. Waste loading of the wasteforms in our research is about 35 wt% (in oxide).

2.2. Microstructure characterization

The glass-ceramic samples were examined in the X-ray powder diffractometer (Cu K_α), and the electron probe approach was used for phase abundances, phase compositions, and grain size, shape and distribution of apatite phase. Quantitative wave length dispersive electron microprobe analyses of both apatites and coexisting glass phases were carried out in the Jxa 8800R microprobe.

In order to maintain consistency in our discussion, bulk compositions for GC_{875} and GC_{500} are obtained by a wet chemical analysis and the electron probe technique, respectively. We continued to use the bulk composition data from the electron probe while making comparison among the subjects involving the data obtained from the electron probe. The bulk composition data obtained from the wet chemical analysis is employed in the discussion about leachability.

2.3. Leaching test

The 28-day static leaching test in MCC-1 test procedures [7] was followed for testing samples of the apatite glass-ceramics GC_{875} and GC_{500} in the deionized water at 90 °C for 3, 7, 14, 28 days. The samples were cut from the corresponding simulated wasteforms as rectangular or trapzoid monoliths. Their surfaces were polished, and the geometric surface areas were measured using a vernier caliper. The samples were contained in tightly closed Teflon containers. The concentrations of dissolved ions in the leachates were determined by inductively coupled plasma-emission (ICP) spectroscopy. The tests were run with a sample surface area-to-solution volume (S/V) ratio of 10 m^2/m^3. The normalized leach rates were calculated as

$$\mathrm{NR}(i) = \frac{m_i}{f_i A d}, \tag{1}$$

where $\mathrm{NR}(i)$ is the normalized leach rate of the element i (g/m^2 day); m_i is the mass weight of the element i in the

leachate (g); f_i is the gross mass fraction of the element i in the multiphase wasteform; A is the surface area of the sample (m^2); and d is the leaching time (day).

3. Discussion

3.1. Characteristics of apatites in the glass-ceramics

The powder XRD pattern (Fig. 1) of the glass-ceramic GC_{875} indicates that apatite was the only crystalline phase and there is also an amorphous phase. Similar XRD patterns occur in the glass-ceramics GC_{825} and GC_{500}. Fig. 1 shows the deconvolution of the spectrum into four chemical variants of apatite, which indicates that apatite with the same structural features as these apatite variants will have a non-stoichiometric composition. The formula derived from the weight-averaged compositions of the deconvoluted apatites is $Sr_{5.5}Ca_{4.5}$-$[P_6O_{24}](OH)_2$.

The back-scattering images of the glass-ceramics also confirm the evidence that the apatite phase distributes in isolated, irregular drops in a glass matrix (see Fig. 2). Area measurements of the apatite drops show that the volume ratios of apatite to glass in GC_{875} and GC_{825} are 52:48 and 48:52, respectively. The volume ratio of

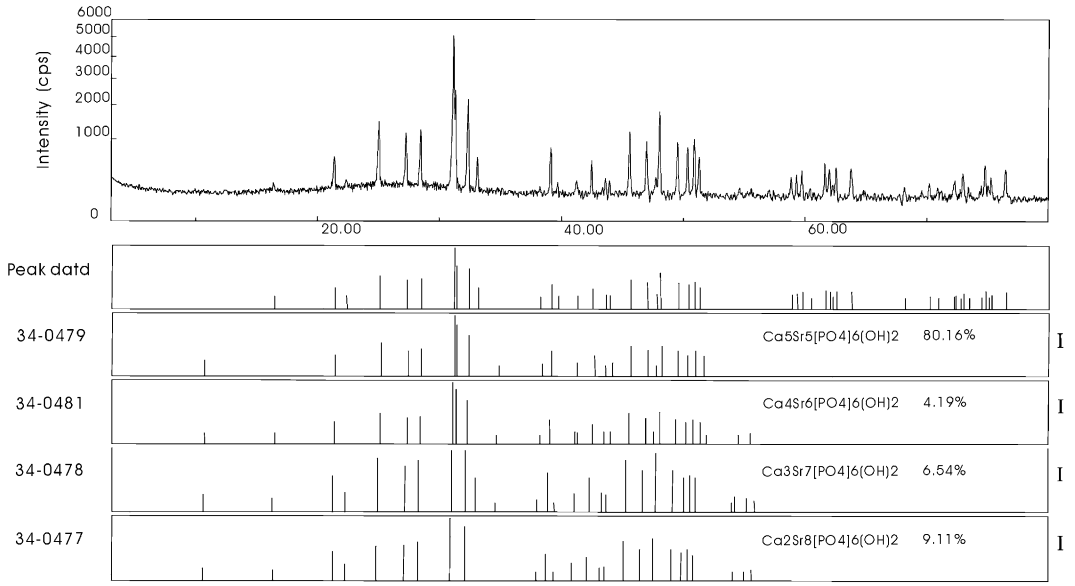

Fig. 1. XRD patterns of the apatite glass-ceramic wasteform GC_{875} and its deconvoluted apatites. The top is the measured XRD spectrum of GC_{875}, and the bottom is XRD line patterns of GC_{875} and its four deconvoluted apatites. The percentage after apatite formula is the mass percentage of this apatite in the apatite of GC_{875}. The numbers on the left of XRD line pattern boxes are JCPDS file numbers of those apatites.

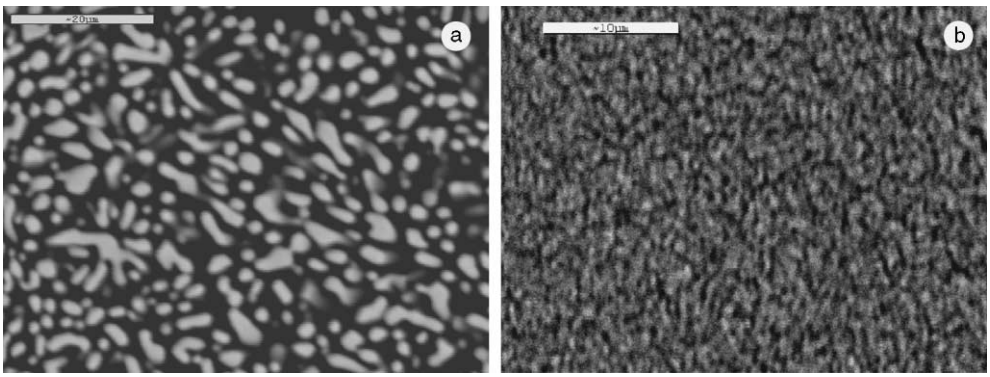

Fig. 2. Back-scattering image of the apatite glass-ceramic wasteforms. (a) A back-scattering image of GC_{875}; (b) A back-scattering image of GC_{500}. Light phase is apatite and dark phase is glass.

apatite to glass for GC_{500} cannot be obtained because of the small size of the grains and the blurred bounderies (see Fig. 2(b)).

The compositions of both the apatite and glass phases in GC_{875}, GC_{825} and GC_{500} were analyzed by using the electron probe, and the results are listed in Table 3. The data for GC_{500}, which is not very reliable because of the small grain size for the electron probe to measure, is used just as a reference to show possible composition evolutions in both the apatite and glass of GC_{500}, GC_{825}, GC_{875}. Apatite formulae calculated from the data in Table 3 are as follows:

$$(Sr_{2.074}Ca_{1.606}Al_{3.277}Si_{0.380}K_{1.295}Na_{0.760}Fe^{2+}_{0.025})[(P_{5.141}Si_{0.839}Mo_{0.020})O_{24}](O_{0.504}F_{0.992}) \quad (2)$$

for GC_{500},

$$(Sr_{3.584}Ca_{2.751}Al_{1.795}Si_{0.266}K_{0.855}Na_{0.476}Fe^{2+}_{0.010})[(P_{5.535}Si_{0.465})O_{24}](O_{0.638}F_{0.724}) \quad (3)$$

for GC_{825},

$$(Sr_{4.552}Ca_{3.558}Al_{0.947}Si_{0.128}K_{0.473}Na_{0.198}Fe^{2+}_{0.010})[(P_{5.741}Si_{0.259})O_{24}](O_{0.634}F_{0.732}) \quad (4)$$

for GC_{875}. These formulae show that the apatite is an oxygen–fluorine apatite in which some O^{2-} ions substitute for F^- ions while some Si^{4+} for P^{5+} in the structure. Comparing the formulae, one can see that the concentrations of the major components Sr, Ca, P increase while the dopants Na, K, Al, Si decrease with the elevation in crystallization temperature, which indicates that perfectly crystallized apatite contains less impurities.

The wet chemical approach was employed to analyze bulk compositions for GC_{875} and GC_{500}. We also analyzed GC_{875}, GC_{875} and GC_{500} by using the electron probe approach and the average results as the bulk composition for the apatite glass-ceramics named GC. Two kinds of the bulk compositions are listed in Table 4. Based on 52 and 48 vol.% apatites in the wasteforms GC_{875} and GC_{825}, 83.3 and 69.8 wt% Sr are immobilized in the apatite phases of GC_{875} and GC_{825}, respectively.

3.2. Characteristics of glass phases in the glass-ceramics

The data in Tables 3 and 4 show that compositions of the glass phases in the apatite glass-ceramics evolve systematically when the crystallization in the glass-ceramics develops gradually with elevating temperatures. From GC_{500} to GC_{875}, the concentrations of Na_2O, K_2O, Al_2O_3, SiO_2, P_2O_5 in the glass phase gradually increased by 17.9, 37.5, 48.8, 44.6 and 8.2 mol%, but the concentrations of SrO and CaO decreased by 55.7 and 59.1 mol%, respectively. The component MoO_3 concentrates entirely in the glass phases of GC_{825} and GC_{875}. Obviously, the GC_{875} glass and GC_{500} glass are quite different.

Table 3
Compositions of apatites and glass matrixes in apatite glass-ceramics (wt%)

Sample	Na_2O	K_2O	FeO	Al_2O_3	CaO	MoO_3	SiO_2	SrO	P_2O_5	F
GC_{500}-apt*	2.33	6.02	0.18	16.53	8.91	0.29	7.25	21.27	36.16	1.86
GC_{500}-glas*	2.24	6.17	0.23	17.44	8.77	0.34	7.51	21.49	36.76	1.75
GC_{875}-apt	0.51	1.84	0.06	3.99	16.50	0.00	1.92	38.99	33.70	1.15
GC_{875}-glas	3.55	9.56	0.44	24.17	3.77	0.34	9.98	8.45	38.47	1.32
GC_{825}-apt	1.30	3.55	0.06	8.07	13.60	0.00	3.87	32.75	34.66	1.21
GC_{825}-glas	3.42	8.53	0.37	21.49	4.95	0.38	8.86	13.05	37.51	1.38

Note: (1) The analyses are carried out by JX Zhou in the Jxa 8800R microprobe. (2) Suffix -apt and -glas mean apatite and glass in the glass-ceramic, respectively. (3) The data with (*) are from single analysis; the others are averages of three replicate analyses.

Table 4
Bulk compositions of apatite glass-ceramics (wt%)

Sample	Na_2O	K_2O	FeO	Fe_2O_3	Al_2O_3	CaO	MoO_3	SiO_2	SrO	P_2O_5	F
GC^*_{875}	3.48	6.53	0.17	0.21	15.08	8.36	0.46	6.78	21.15	36.25	1.44
GC^*_{500}	3.47	6.56	0.15	0.23	15.08	8.16	0.48	6.78	21.10	36.04	1.91
GC	3.01	6.95	0.23	–	16.24	8.51	–	6.90	20.65	35.54	–

Note: (1) The data with (*) are from the wet chemical analysis. (2) The data for GC are averages of electron probe data from GC_{875}, GC_{825} and GC_{500}. (3) '–' Means no detection.

3.3. Leachability

Following the 28-day static leaching test procedure in MCC-1, two sets of monolithic samples were cut from the two glass-ceramic wasteforms, i.e. GC_{875} and GC_{500}, respectively. Their surface areas range between 499 and 590 mm^2. Each set consists of six monolithic samples, of which three samples were for 3-day, 7-day, and 14-day leaching tests, respectively, and three samples for a 28-day leaching test. Two blanks only with deionized water are for the 28-day test. When each test ended, the monolithic sample was examined under a stereo microscope. No changes on the samples were observed. The weight losses for the GC_{875} monoliths are 0.17 mg per day for the 3-day test, 0.34 mg/day for the 7-day test, 0.11 mg/day for the 14-day test, and 0.06 mg/day for the 28-day tests. For the GC_{500} monoliths, the weight losses are 0.13 mg/day for the 3-day test, 0.31 mg/day for the 7-day test, 0.07 mg/day for the 14-day test, and 0.05 mg/day for the 28-day tests. Leachates were analyzed by the ICP technique. Only are components Ca and K detected in the blanks and have the average concentrations of 1.0876 and 0.0126 μg/ml, respectively, which should be removed as background concentrations from the concentrations of the corresponding components in the leachates while calculating the normalized leach rates. The normalized leach rates for the relevant elements of the two sets of samples are listed in Table 5. The negative sign indicates that Ca is adsorbed by the monoliths instead of leaching from them in all the leach tests. The term m_i in the Eq. (1) is replaced by the term (m_i – the average of Ca in the blanks) while calculating the normalized adsorbing rates for Ca. Concentrations of Na were not obtained because of an error in making the profile.

From Table 5, it is evident that elements K, Sr, Al, P appear in all leach tests for both GC_{875} and GC_{500}; elements Mo and Si are found in all 28-day leach tests for GC_{875}, and occasionally in separate 28-day leach tests for GC_{500}. The component Fe is not detectable in all leach tests for GC_{500}, but it appears in one leachate of 28-day tests for GC_{875}. The leach rates of above elements in GC_{875} are all higher than those in GC_{500}. At the 3-day tests, the GC_{500} monolith adsorbs more Ca than GC_{875}, but the normalized adsorbing rates of Ca for both GC_{500} and GC_{875} become much close to each other at the 28-day tests (see Fig. 3).

Fig. 3 shows the plots of the normalized leach rates for relevant elements and the normalized adsorbing rates for Ca versus the leaching times. Comparing Fig. 3(a) with (b), one can find that the leach patterns of the elements K, Al, P in GC_{500} and GC_{875} resemble each other, that the leach rates of K, (Al, P) and Sr drop essentially in order of 10^{-1} successively, and that Al and P leach in the same order of magnitude. Leach behavior of Sr in GC_{875} presents a phenomenon of reprecipitation in Fig. 3(b).

Table 5
Normalized adsorbing rates of Ca and normalized leach rates of the other elements in apatite glass-ceramics (g/m^2 day)

Sample	Time (day)	Ca	K	Sr	P	Al	Si	Mo	Fe
GC_{875}	3	-3.70×10^{-1}	3.19×10^{-1}	1.00×10^{-2}	1.13×10^{-1}	9.43×10^{-2}	nd	nd	nd
	7	-2.28×10^{-1}	3.21×10^{-1}	5.60×10^{-3}	8.19×10^{-2}	1.21×10^{-1}	nd	nd	nd
	14	-1.19×10^{-1}	1.94×10^{-1}	5.70×10^{-3}	5.22×10^{-2}	5.99×10^{-2}	nd	nd	nd
	28	-6.29×10^{-2}	2.40×10^{-1}	1.20×10^{-3}	6.78×10^{-2}	5.84×10^{-2}	1.06×10^{-1}	5.03×10^{-2}	nd
	28	-6.34×10^{-2}	1.89×10^{-1}	9.00×10^{-4}	4.90×10^{-2}	5.54×10^{-2}	5.00×10^{-2}	1.15×10^{-2}	nd
	28	-6.33×10^{-2}	1.72×10^{-1}	8.00×10^{-4}	4.91×10^{-2}	4.27×10^{-2}	6.11×10^{-2}	1.46×10^{-2}	1.56×10^{-2}
	Average (28)	-6.32×10^{-2}	2.00×10^{-1}	9.70×10^{-4}	5.53×10^{-2}	5.22×10^{-2}	7.24×10^{-2}	2.55×10^{-2}	5.20×10^{-3}
GC_{500}	3	-6.17×10^{-1}	1.67×10^{-1}	1.40×10^{-3}	2.52×10^{-2}	2.34×10^{-2}	nd	nd	nd
	7	-2.56×10^{-1}	2.07×10^{-1}	1.50×10^{-3}	4.81×10^{-2}	7.36×10^{-2}	nd	nd	nd
	14	-1.26×10^{-1}	8.21×10^{-2}	5.00×10^{-4}	1.85×10^{-2}	1.14×10^{-2}	nd	nd	nd
	28	-6.46×10^{-2}	8.60×10^{-2}	4.00×10^{-4}	2.27×10^{-2}	2.98×10^{-2}	nd	8.1×10^{-3}	nd
	28	-5.79×10^{-2}	9.08×10^{-2}	8.00×10^{-4}	2.21×10^{-2}	2.19×10^{-2}	nd	nd	nd
	28	-6.15×10^{-2}	1.49×10^{-1}	8.70×10^{-4}	4.03×10^{-2}	4.50×10^{-2}	3.26×10^{-2}	nd	nd
	Average (28)	-6.13×10^{-2}	1.09×10^{-1}	6.90×10^{-4}	2.84×10^{-2}	3.22×10^{-2}	1.09×10^{-2}	2.70×10^{-3}	nd

'nd' indicates not detectable. ICP analyses were carried out by RX Xin.

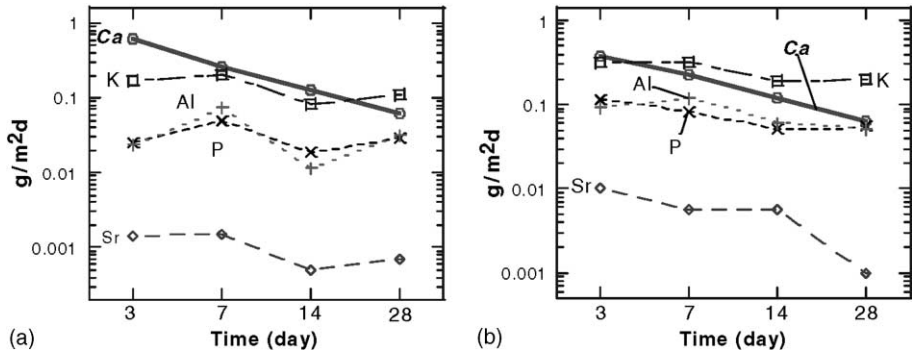

Fig. 3. Plots of leaching times versus the normalized adsorbing rates of Ca and normalized leach rates of the other elements in simulated wasteforms. (a) is for GC_{500} and (b) is for GC_{875}.

Table 6
Comparison of normalized leach rates of corresponding elements among GC_{500} and several wasteforms (g/m^2 day)

Wasteform	Sr	Mo	K	Al	Ca	Si	P	Remark
B–Si Glass-1	1.5					1.0		[2]
B–Si Glass-2	0.5		0.5	1.0	0.35	0.33	0.78	14-day-test, [8]
B–Si GC	0.3		0.29	0.34	0.11	0.3	0.04	14-day-test, [8]
Synroc-C	0.002	0.05		0.0001	0.006		0.08	[9]
Fe–P Glass					0.0068	0.0062	0.00095	[10]
NZP-C	0.1	2.0		0.002	0.2		0.1	[9]
Monazite-C	0.0015						0.00075	[2]
GC_{500}	0.00069	0.0027	0.09	0.032	−0.061	0.011	0.028	This work

Note: B–Si Glass-1 and -2 are borosilicate glasses; B–Si GC is a borosilicate glass-ceramic; Fe–P Glass is an iron phosphate glass; NZP-C is a sodium zirconium phosphate ceramic; Monazite-C is a monazite ceramic.

As we know from the crystal chemistry, a well crystallized crystal tends to contain as few impurities as possible and, therefore, it possesses the lowest lattice energy and the highest stability. Hence, the apatite in GC_{875} should be more stable than one in GC_{500}. Supposing that the apatites in GC_{500} and GC_{875} have equivalent stability, then the difference in leach behavior between GC_{500} and GC_{875} should be attributed mainly to their different glass phases. The apatite glass-ceramic GC_{500} containing poorly crystallized apatite with a lot of impurities possesses higher chemical stability than GC_{875}. Based on our research, the optimum microstructure for the apatite glass-ceramic wasteform should be poorly crystallized apatite with a lot of impurities distributed evenly in a glass matrix with similar composition.

The normalized leach rates of corresponding elements in several known wasteforms are listed in Table 6 in order to make a comparison to the leach rates of GC_{500}. From this comparison, it is evident that the apatite glass ceramics have effectively immobilized Sr as a host for Sr HLLW. Among the waste components, i.e., Sr, K, Mo, and Al, only the leach rate of Al in GC_{500} is higher than those of NZP ceramic and Synroc-C. Among the additives, the leach rate of P in GC_{500} is higher than that of P in the other two phosphate wasteforms, and the leach rate of Si in GC_{500} is higher than in iron phosphate glass. The low normalized leach rate of the GC_{500} Mo indicates that the apatite glass-ceramics would be a workable host candidate for immobilizing Mo-rich HLLW, even though the mass concentration of Mo in the apatite glass-ceramics is quite low.

4. Conclusion

The low leach rates of Sr show that the apatite glass-ceramics as a wasteform for a Sr HLLW have effectively immobilized Sr. The leach behavior of Mo in the leaching tests indicates that this wasteform is a candidate for Mo-rich HLLW. From our research, it is evident that the leach rates of the elements are strongly influenced by the properties of both the elements themselves and their hosts, but not so much by their gross mass concentrations in the hosts. For example, the leach rates of all the elements increase, but the leach patterns of the relevant elements do not change very

much when the glass composition in GC_{500} evolves to that in GC_{875}. Component Ca does not leach at all from the testing samples, but is adsorbed by them. The adsorbing rates of Ca decrease with the increase of testing time. As a glass-ceramic wasteform, the effects of crystallization on its leach rates cannot be ignored. A perfect crystallization should make the crystal phase more stoichiometric, which significantly changes the composition of coexisting glass phase in the system, as in our case. For an apatite glass-ceramic wasteform, the optimum microstructure should be one in which poorly crystallized apatite crystallites distribute evenly in the coexisting glass phase.

Acknowledgements

One of the authors, Y.H., thanks the China Scholarship Council and the Laboratory for Studies in Geological Waste Disposal and Environment Protection, Hubei, People's Republic of China (Project: HBWDED-2000-01) for partial financial support.

References

[1] W. Donald, B.L. Matcalfe, R.N.J. Taylor, J. Mater. Sci. 32 (1997) 5851.
[2] L.A. Boatner, B.C. Sales, Monazite, in: W. Lutze, R.C. Ewing (Eds.), Radioactive Waste Form for the Future, Elsevier Science, North Holland, 1988, p. 495.
[3] P. Wang, Z.L. Pan, L.B. Wong, in: System Mineralogy, vol. 2, Geology, Beijing, 1984, p. 207 (in Chinese).
[4] P. Wang, Z.L. Pan, L.B. Wong, in: System Mineralogy, vol. 3, Geology, Beijing, 1987, p. 132 (in Chinese).
[5] Y. He, Radiat. Protect. 21 (1) (2001) 43 (in Chinese).
[6] C.L. Song, Sci. Technol. Nucl. Energy 29 (1995) 201 (in Chinese).
[7] MCC, Nuclear waste materials handbook. (Materials Characterization Center, Hanford, WA), Report No. DEC/TIC-11400, 1983.
[8] S.V. Raman, J. Non-Cryst. Solids 263&264 (2000) 395.
[9] V.N. Zyryanov, E.R. Vance, Comparison of sodium zirconium phosphate-structured HLW forms and Synroc for high-level nuclear waste immobilization. Material Research Society Symposium, Boston, MA, 1996.
[10] G.K. Marasinghe, M. Karabulut, C.S. Ray, et al., J. Non-Cryst. Solids 263&264 (2000) 146.